01 Feb 2008

Charge Exchange and X-Ray Emission Cross Sections for Multiply Charged Ions Colliding with H_2O

Sebastian Otranto
Missouri University of Science and Technology, otrantos@mst.edu

Ronald E. Olson
Missouri University of Science and Technology, olson@mst.edu

Recommended Citation

S. Otranto and R. E. Olson, "Charge Exchange and X-Ray Emission Cross Sections for Multiply Charged Ions Colliding with H_2O," *Physical Review A*, American Physical Society (APS), Feb 2008.
The definitive version is available at https://doi.org/10.1103/PhysRevA.77.022709

Charge exchange and x-ray emission cross sections for multiply charged ions colliding with H_2O

S. Otranto[1,*] and R. E. Olson[2]
[1]*CONICET and Dto. de Física, Universidad Nacional del Sur, 8000 Bahía Blanca, Argentina*
[2]*Physics Department, University of Missouri-Rolla, Rolla, Missouri 65401, USA*
(Received 7 December 2007; published 20 February 2008)

Total and state selective *nl*-electron capture cross sections are presented for highly charged ions $Z=4-10$, 14, 18, and 26 colliding with water molecules. The energy range investigated was from 10 eV/amu ($v=0.02$ a.u.) to 100 keV/amu ($v=2$ a.u.). An initialization for the $1B1$ and $3A1$ orbitals of the water molecule is introduced based on the one center expansion of Moccia and compared to our previous studies based on a hydrogenic approximation within the microcanonical ensemble. The Z dependence of the calculated total cross sections is in reasonable agreement with the recent data of Mawhorter *et al.* [Phys. Rev. A **75**, 032704 (2007)] and is improved over previous results. The energy dependence of the n- and l-level populations is investigated. The K-shell x-ray emission cross sections are determined by using the calculated state-selective electron capture results as input and then applying hydrogenic branching and cascading values for the photon emission. Our results compare favorably with experimental data from the KVI-Groningen, Jet Propulsion Laboratory and Lawrence Livermore National Laboratory groups.

DOI: 10.1103/PhysRevA.77.022709 PACS number(s): 34.70.+e, 32.30.Rj, 32.70.Fw, 95.30.Ky

INTRODUCTION

State-selective single electron capture (CX) induced by highly stripped multiply charged ions colliding with atoms and molecules in general produces an excited ion that decays via photon emission. The resulting spectra are extremely sensitive to how the different n,l states for the projectile are populated during the charge exchange reaction. As such, the study of these collision systems provides a severe test for theoretical models which in general face a twofold problem: computation times that for high-Z projectiles are prohibitive and the determination for the description of complex reactants such as molecular targets.

For collision energies $E<100$ keV/amu, several theoretical methods have been used to estimate the capture cross sections. Quantum mechanical techniques such as the atomic and molecular orbital methods provide accurate values for systems where the basis sets can be of reasonable size, such as low-charged projectiles and light atomic targets like H and He at energies where the ionization continuum is unimportant [1,2]. Albeit other much simpler methods, such as the multichannel Landau-Zener (LZ) [3] and classical trajectory Monte Carlo (CTMC) methods [4,5], allow greater flexibility and provide general scaling relationships for molecular targets or high charge state projectiles [6].

The LZ and CTMC methods early on predicted that the total cross sections for CX with hydrogen targets scaled linearly with charge state at intermediate energies and were independent of energy for high charge state projectiles, with a magnitude of roughly $\sigma\sim Z\times 10^{-15}$ cm^2 [3,7,8]. Furthermore, CTMC calculations showed that the most probable principle quantum number for capture scales as $q^{3/4}$ [9]. This result was also later derived within the framework of the classical over-the-barrier model [10].

Even though the total and n-selective cross sections can be qualitatively predicted by different methods, the l orbital angular momentum levels produced by electron capture are elusive. In general, the l levels tend to have statistical populations proportional to $2l+1$, at the higher energies, while low values of l dominate for very slow collisions [9]. An accurate description of this energy dependence is crucial for the determination of the line emission cross sections at intermediate collision energies since the photon branching ratios are directly tied to the initial *nl* distributions.

The experimental work in this field has grown considerably in recent years, motivated by observations of x-ray emission from comets as they transit our solar system. This CX driven process was discovered in 1996 by means of the ROSAT satellite and since then, x-ray emission from more than 15 comets have been analyzed by this and other satellites. It is now recognized that the x rays arise from electron capture collisions between multiply charged ions in the solar wind and the gases, primarily H_2O, surrounding the comet [11]. The energy range of interest for the colliding "solar wind ions" is approximately 0.8 keV/amu to 3.0 keV/amu, corresponding to the slow and fast components of the solar wind. From the astrophysical data, it is inferred that the solar wind ions that dominate soft x-ray emission are primarily high charge states of carbon and oxygen.

To gain insight into these charge exchange reactions, laboratory-based work has been performed for systems of astrophysical interest and complementary sets of data have been obtained by at least four independent groups. Work at the Jet Propulsion Laboratory (JPL) has focused on the determination of the CX total cross sections and the x-ray emission lines for highly charged ions of C, N, O, and Ne colliding on H_2O, He, H_2, and CO_2 at collision energies which are representative of those corresponding to the solar wind ions [12,13]. Work at the Lawrence Livermore National Laboratory (LLNL) has used an electron beam ion trap (EBIT) with a microcalorimeter detector to measure very high resolution x-ray data for O^{8+} collisions on CO_2, CH_4, N_2, He, and alcohol. Other measurements have employed a SiLi detector and have investigated bare and H-like Ne collisions on Ne, Fe on N_2, Ar on Ar, and Kr on Kr. The EBIT

*sotranto@uns.edu.ar

work was conducted at an energy of ~10 eV/amu, which is two orders of magnitude lower than those observed for the solar wind ions [14–17]. Experiments at KVI-Groningen have investigated collisions that emit photons in the EUV range such as He^{2+} on H_2O, CO, CO_2, CH_4, and O^{6+} on H_2O [18,19]. Further experimental work at Belfast was focused on O^{6+} collisions with H_2O, CO_2, CH_4, and C^{4+} on CH_4 by means of the Translational Energy Spectroscopy (TES) technique [20]. There is also related work in the field which was carried out with the NIST EBIT (H-like and He-like Ne, Ar, and Kr ions on Ar) [21] and the Berlin EBIT (Ar^{18+} on Ar) [22].

From the theoretical point of view, astrophysical models for electron capture reactions have assumed equal population of the l values, or statistical populations where the ion deexcites via photon cascades along the yrast chain $\Delta n=-1$ that primarily produces just the Lyman alpha line in the x-ray region [23–25]. There are also Landau-Zener calculations with the l values adjusted to reproduce available data [26,27]. A parameter-free approach is provided by the CTMC model which inherently yields the l-states distribution without invoking any physical limit or *ad hoc* procedure. Recent studies have shown that this method is capable of providing qualitative agreement with laboratory CX cross sections and line emission cross sections at varying impact energies. Furthermore, the CTMC emission lines convoluted over the spectrometer's effective area and energy resolution compare satisfactorily with the satellite spectra for comets LINEAR C/1999 S4 and McNaught-Hartley C/1999 T1 [28–30] obtained from the Chandra X-ray Observatory (CXO) satellite.

Line emission cross sections calculated using the CTMC method for the atomic hydrogen targets have a long history. They are used as the basis for diagnostics on tokamak fusion plasmas to determine the concentrations of impurity ions, A^{q+} [31,32]. The spectra themselves are further used as a diagnostic to estimate the plasma temperature by measuring the broadening of the specific spectral lines, along with determining the plasma rotation via the Doppler shift of the lines. However, the CTMC calculations have generally been applied at intermediate collision energies, 1–40 keV/amu, because these energies correspond to the injection energy of tokamak fueling and heating H or D neutral beams, along with the atoms slowing down due to collisions with the plasma components.

In this paper, we study the CX cross sections as well as the line emission cross sections resulting from the collision of ions with $Z=4-10$, 14, 18, and 26 on H_2O molecules. These systems were chosen because of their direct relevance to x-ray emission from comets and to provide a broad range of Z values to determine scaling information. In Sec. II, the initialization procedure for the active electron is introduced and compared to the usual hydrogenic approximation used in our previous studies. The present results are then compared to the available experimental data as well as to our previous results in Sec. III. Finally, conclusions and outlook are drawn in Sec. IV.

THEORETICAL METHOD

We have performed classical trajectory Monte-Carlo (CTMC) calculations of the cross sections for single electron capture [4,5]. Hamilton's equations were solved for a mutually interacting three-body system. While bare ions are represented by means of Coulomb potentials, for partially stripped ions the active electron is considered to evolve under the potential model developed by Green *et al.* from Hartree-Fock calculations [33] that was generalized by Garvey *et al.* [34]. The CTMC method directly includes the ionization channel and is not limited by basis set size for the prediction of capture to very high-lying excited states.

A classical number n_c is obtained from the binding energy E_p of the electron relative to the projectile by

$$E_p = -Z_p^2/(2n_c^2), \tag{1}$$

where Z_p is the charge of the projectile core. Then, n_c is related to the quantum number n of the final state by the condition

$$[(n-1)(n-1/2)n]^{1/3} \leqslant n_c \leqslant [n(n+1)(n+1/2)]^{1/3}. \tag{2}$$

From the normalized classical angular momentum $l_c = (n/n_c)(\mathbf{r}\times\mathbf{k})$, where $\mathbf{r}$ and $\mathbf{k}$ are position and momentum of the captured electron relative to the projectile, we relate l_c to the orbital quantum number l of the final state by

$$l \leqslant l_c \leqslant l+1. \tag{3}$$

The m_l determination is satisfied by

$$\frac{2m_l-1}{2l+1} \leqslant \frac{l_z}{l_c} \leqslant \frac{2m_l+1}{2l+1}, \tag{4}$$

where l_z is the z projection of the angular momentum obtained from the calculations [35].

The cross section for a definite (n,l,m) state is then given by

$$\sigma_{nl} = N(n,l,m)\pi b_{\max}^2/N_{\text{tot}}, \tag{5}$$

where $N(n,l,m)$ is the number of events of electron capture to the nlm level and N_{tot} is the total number of trajectories integrated. The impact parameter $b_{\max}$ is the value beyond which the probability of electron capture is negligibly small.

In order to obtain emission cross sections $\sigma^{(\text{em})}_{n,l,m\to n',l',m'}$, cascade contributions from higher $n''>n$ levels are included and the n,l,m_l populations are multiplied by hydrogenic branching ratios $b_{l\to l'}$ for the relevant transitions [36] and by their relative line strengths [35].

Concerning molecular targets, only the H_2 target has so far been formulated for application to the CTMC method [37]. In previous articles we considered the hydrogenic approximation to be valid for molecules in which a particular reactant was represented by a hydrogen atom ($Z=1$) with an ionization potential appropriate for the molecule under study. Furthermore, the position and momentum vector components were distributed according to the microcanonical distribution

$$f(\mathbf{r},\mathbf{p}) = k\delta[E_i - p^2/2\mu - V(r)],$$

where E_i is the ionization potential and k a normalization constant.

It has been stated for years that the success of the CTMC model for light targets can be associated with the fact that the microcanonical distribution leads to the exact quantum me-

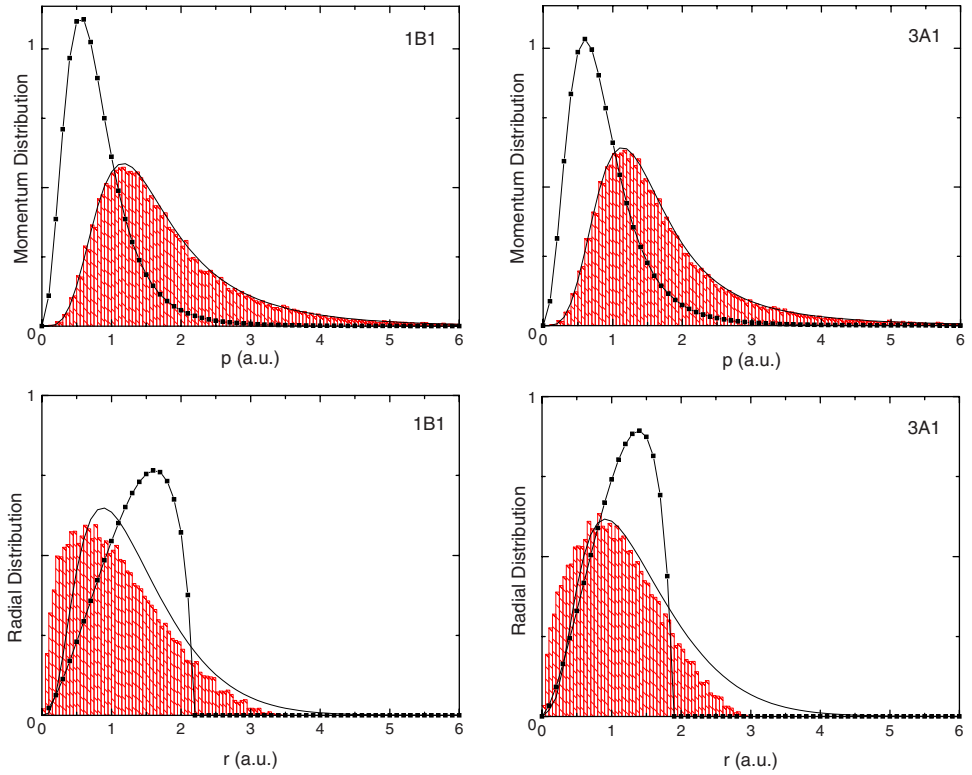

FIG. 1. (Color online) Momentum and radial distributions for the $1B1$ and $3A1$ orbitals. Solid line: Quantum mechanical distributions obtained from Moccia's orbitals; columns: present mCTMC model; line with solid squares: microcanonical-hydrogenic CTMC ($Z_{\text{eff}}=1$).

chanical momentum distribution for the H target. Moreover, for the He target the quantum mechanical momentum distribution is almost identical to that obtained within the microcanonical ensemble when proper model potentials are employed for the latter [38–40]. On the other hand, for molecular targets such as H_2O the hydrogenic approximation leads to momentum and radial distributions that are in disagreement with their quantum mechanical counterparts. Since charge exchange processes are strongly dependent on the target-projectile phase space matching, we are led to conclude that an improvement over the hydrogenic approximation is clearly needed.

To accommodate this fact, we have used a one-center expansion in terms of Slater functions proposed by Moccia [41] to represent the different H_2O orbitals. From these wave functions we have obtained the corresponding "quantum mechanical" momentum and radial distributions associated with each orbital. In our CTMC method, we have sorted the initial momentum p value over the Moccia's momentum distribution for each orbital and have used the energy conservation relationship to obtain the corresponding r value. This r value depends on the choice of the electron-target core interaction which is assumed to be Coulombic with an effective charge Z_{eff}. The effective charge has been set in order to provide the closest possible agreement between the quantum mechanical and classical radial distributions. We refer to this model as the mCTMC method.

In the present treatment, we have explicitly considered the $1B1$ and $3A1$ orbitals of the H_2O molecule with their ground state binding energies of 12.6 eV and 14.7 eV, respectively. We have not included the $1B2$ orbital with a binding energy of 18.5 eV because the electron capture data of Richardson *et al.* [42] for protons colliding with H_2O indicates that the latter makes a negligible contribution to the cross section. We have used branching ratios of $\frac{1}{2}$ each for the $1B1$ and $3A1$ molecular orbits, which are consistent with the proton CX data. The resulting radial and momentum distributions

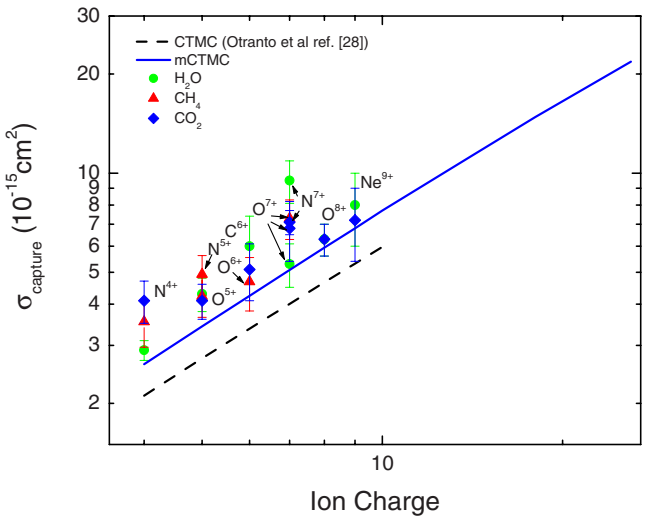

FIG. 2. (Color online) Total single electron capture cross sections in 7 q keV collisions of O^{q+}, N^{q+}, and Ne^{q+} on H_2O, CO_2, and CH_4 targets as a function of the projectile charge [13,43]. The mCTMC results are for 1 keV/amu.

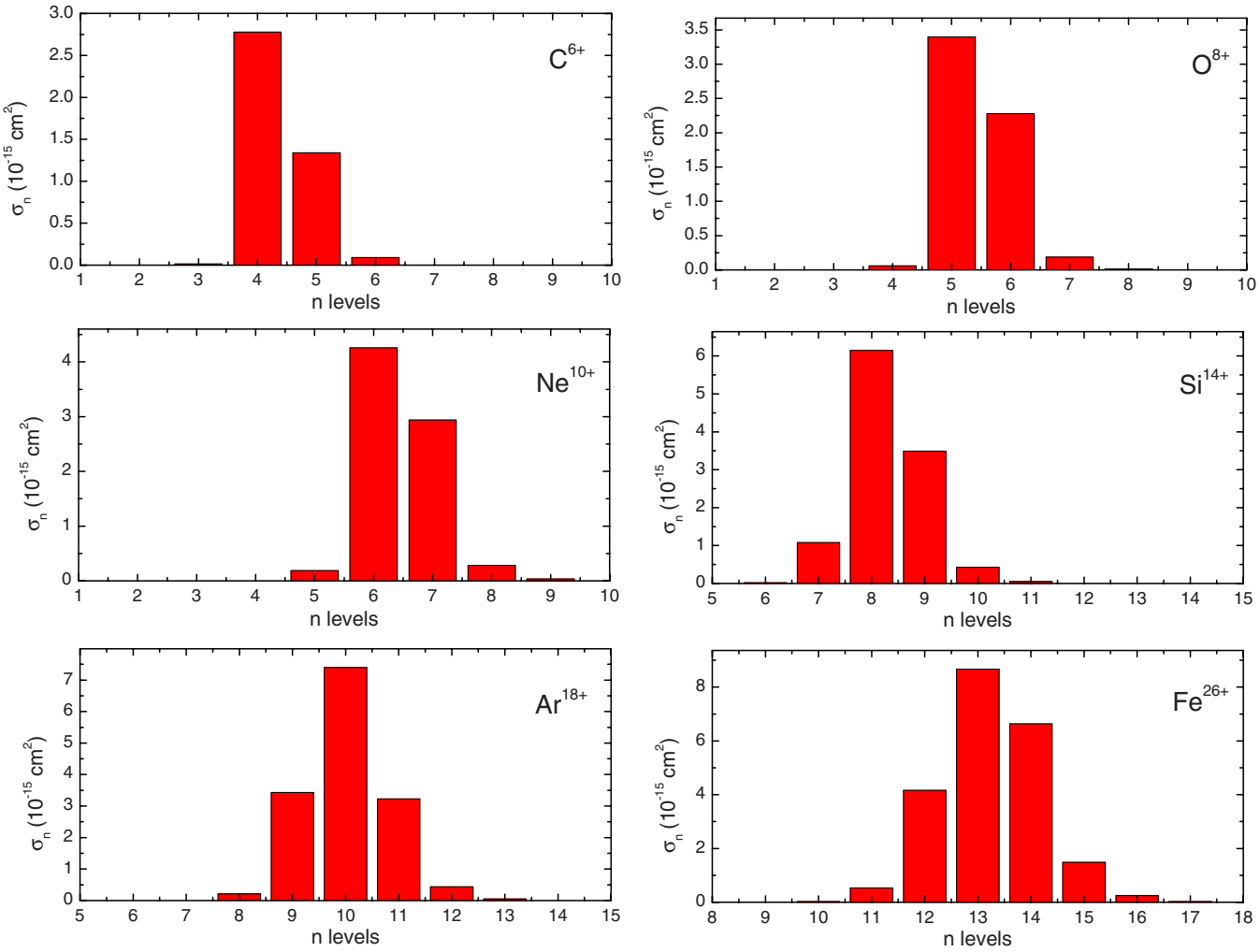

FIG. 3. (Color online) n-state selective single electron capture cross sections for 1 keV/amu ions impinging on H_2O.

are shown and compared in Fig. 1. The explicit value $Z_{\text{eff}}=1.6$ has been used for both the $1B1$ and the $3A1$ orbitals. The present initialization is found to considerably improve the momentum as well as the radial distributions when compared to the microcanonical, hydrogenic approximation. It is important to note that $Z_{\text{eff}}=1.6$ is used only for the interaction between the target nucleus and its electron. The interactions of the projectile with the target nucleus and electron are maintained at their unscreened values so that there is no artificial acceleration, or deceleration, of the projectile toward the target in very slow collisions.

RESULTS

In this section, we will begin with the total cross sections, then systematically proceed to higher levels of the various partial cross sections. For the total cross sections, data exists from the JPL experimental group. In their work, CX total cross sections for different ions colliding with H_2O, CH_4, and CO_2 have been tabulated and compared to classical over-the-barrier (COB) model predictions as well as to our previous results [13,43]. In Fig. 2, 1 keV/amu mCTMC results are compared to the data as well as to our previously published results. We observe an increase in the total cross sections of about 20–30 % compared to the hydrogenic model. It is well known for hydrogen targets that the total cross section scales linearly with the projectile charge ($\sigma \sim Z \times 10^{-15}$ cm^2) [3,7,8]. A similar trend is shown by the data for the molecular targets considered and is followed by our H_2O calculations. We have observed a very slight deviation from a linear law. A nonlinear fit in the range of projectiles charges ($Z=4-26$ at 1 keV/amu) considered in this mCTMC work yields $\sigma=(a\times Z^b)\times 10^{-15}$ cm^2 with $a=0.58\pm0.02$ and $b=1.11\pm0.01$. The exponent deviates slightly from unity and reflects the varying contributions of the molecular states used in the calculations.

Our single capture CX cross sections systematically underestimate the data by approximately 25%. One should expect such a trend since a fraction of the observed single electron capture by the projectile arises from double capture followed by Auger emission of one of the electrons before the projectile is detected. Coincidence measurements of the projectile and target charge states indicate that the fraction of double capture autoionizing to single capture events can be as high as 30–40 % for the heavier rare gas targets such as Ar and Xe. In these latter cases, there is the maximum number

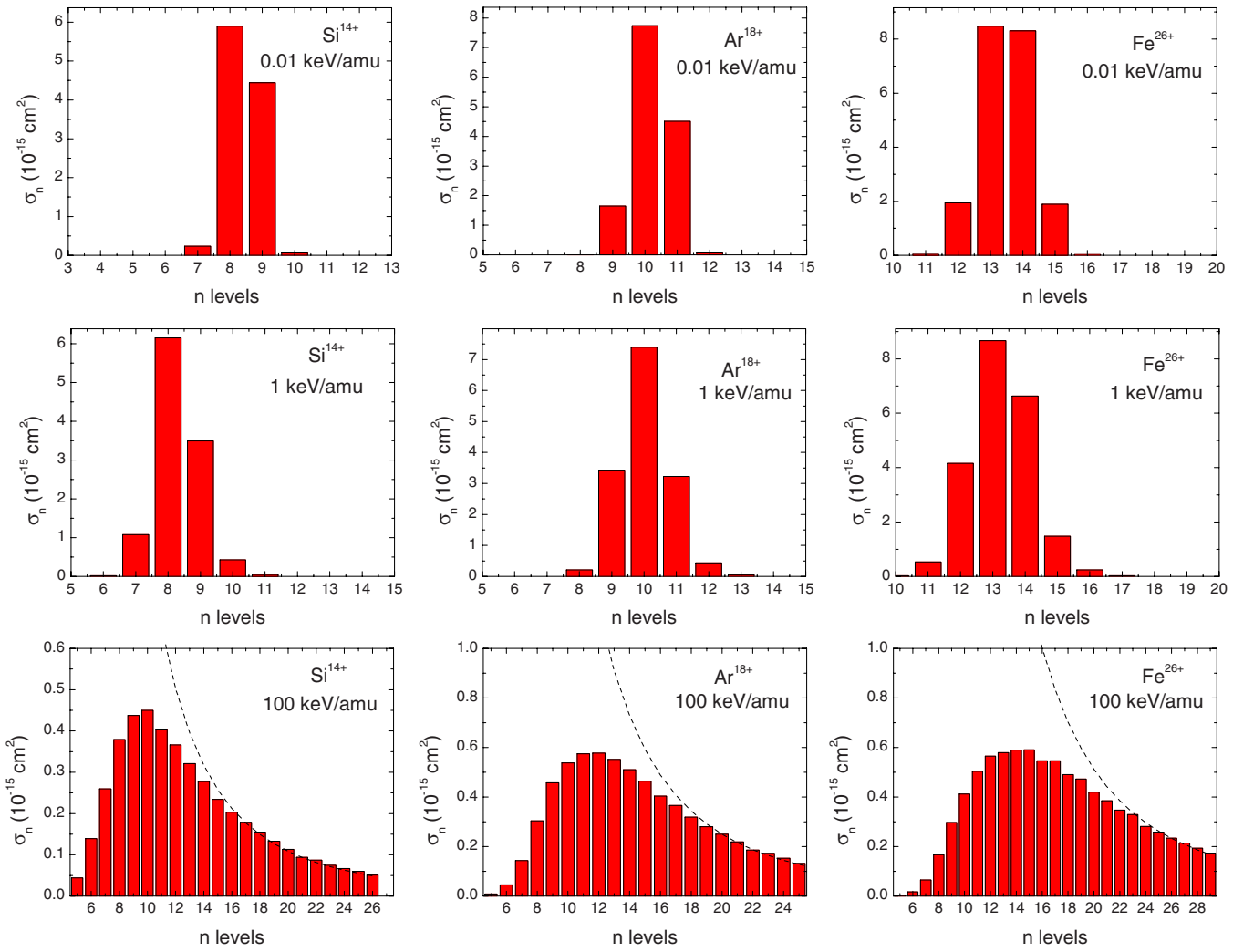

FIG. 4. (Color online) n-state selective single electron capture cross sections for 0.01, 1, and 100 keV/amu Si^{14+}, Ar^{18+}, and Fe^{26+} ions impinging on H_2O.

of electrons in the outer shell available for double capture with sequential binding energies rising less sharply then for lighter targets such as H_2O. We expect the double capture with Auger fraction for H_2O is less than for the heavy rare gas systems since the single ionization potential of H_2O is $\sim$14 eV, while the double ionization threshold is approximately 41.4 eV.

Proceeding to the partial cross sections, in Fig. 3 are shown the n-state electron capture cross sections for C^{6+},O^{8+}, Ne^{10+}, Si^{14+}, Ar^{18+}, and Fe^{26+} collisions on H_2O at an collision energy of 1 keV/amu. In agreement with our hydrogenic results [30], the present distributions closely peak according to the $(13.6\ \mathrm{eV}/\mathrm{IP}_{\mathrm{target}})^{1/2}q^{3/4}$ scaling [9] predicted previously, after one considers the target ionization energies used in the calculations.

To investigate the energy dependence of the n-state partial cross sections, a similar analysis is shown in Fig. 4 for Si^{14+}, Ar^{18+}, and Fe^{26+} ions impinging on H_2O at collision energies of 0.01, 0.1, and 10 keV/amu. Such an analysis has not been given before for such high charge states. To emphasize any energy dependence, the calculations span four orders of magnitude. We find that the n distributions broaden considerably above 1 keV/amu. At 100 keV/u there is a slight shift in the maxima to higher n levels. This is due to the increasing importance of electron removal to the ionization channel, rather than to electron capture. Ionization is removing flux from the stronger collisions that, at the lower energies, preferably populate the more tightly bound low-n capture states.

In Fig. 4, we have added a dashed curve indicating the $\propto n^{-3}$ scaling expected for the population of large n values. This behavior already predicted by Oppenheimer in 1928 should be expected for high impact energies and, as a result, it can be seen that only the 100 keV/u results follow this dependence. Such behavior can only be expected when the ionization channel is strong enough as to lead to a constant value for dQ/dE. In this situation, the n^{-3} behavior for the high-lying capture levels can be derived by recalling simple density of states arguments.

Although the n-level partial cross sections are relatively invariant with collision energy, as shown in Fig. 4, the nl-level cross sections are extremely sensitive to the collision energy. Of course, this sensitivity makes it a challenge to

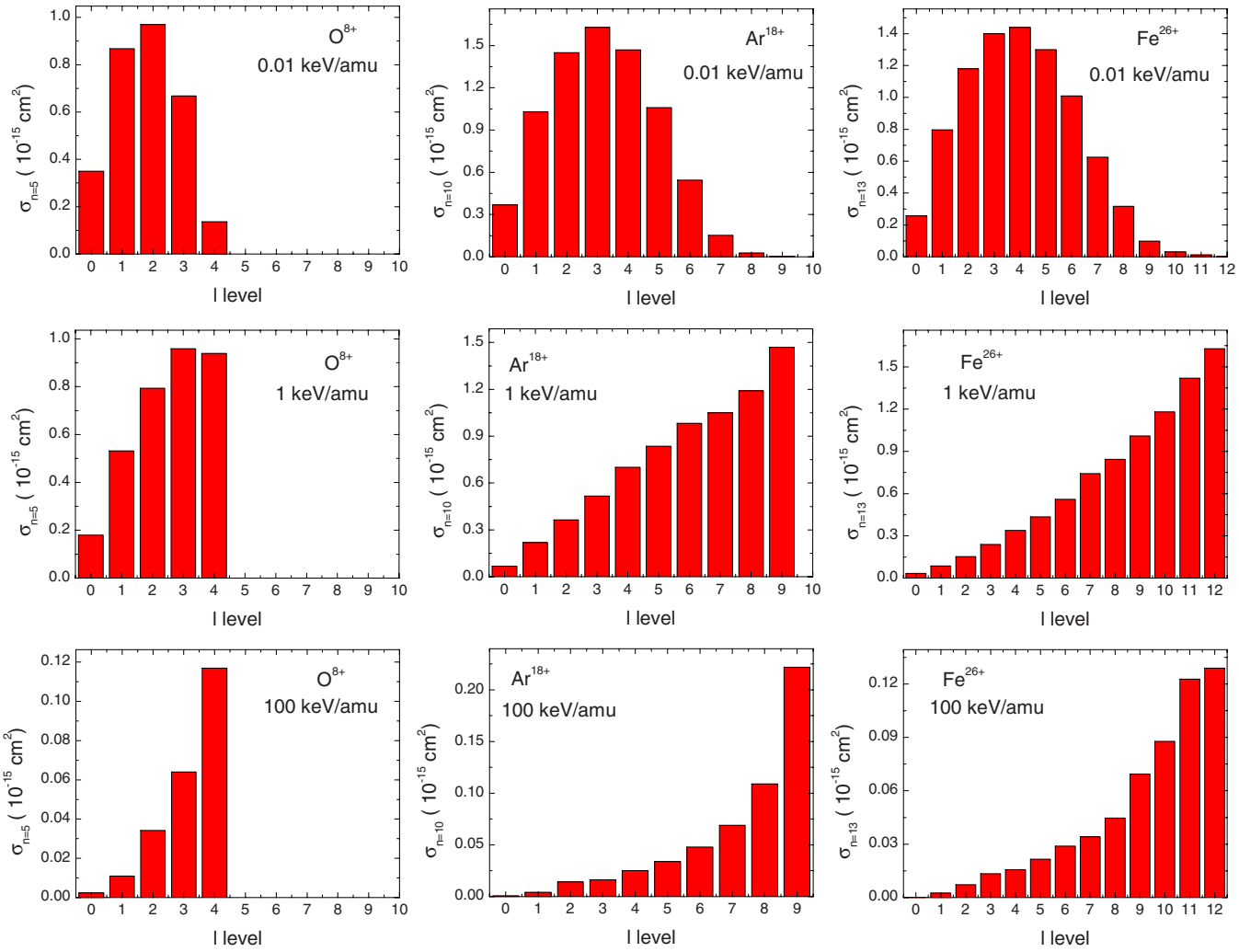

FIG. 5. (Color online)*l*-state selective single electron capture cross sections for 0.01, 1, and 100 keV/amu O^{8+}, Ar^{18+}, and Fe^{26+} ions impinging on H_2O.

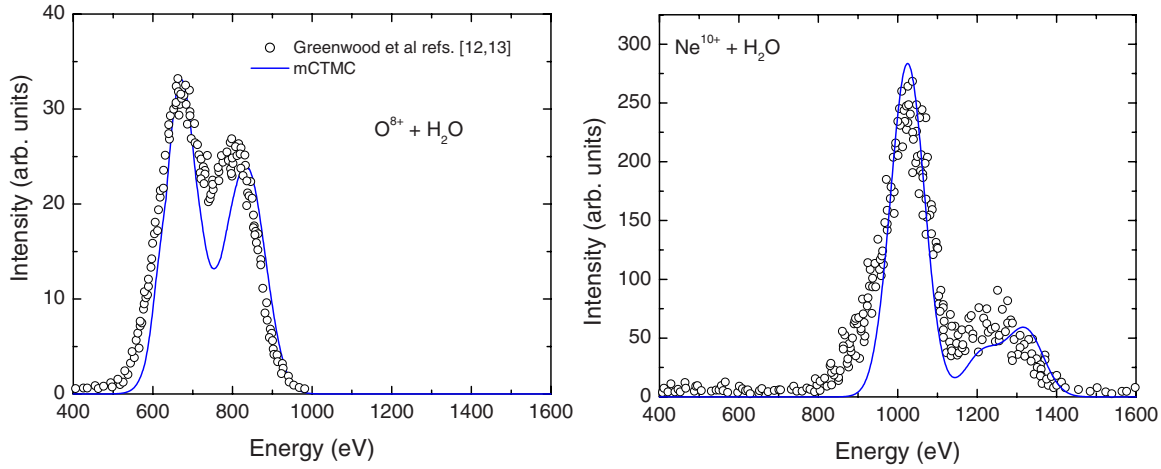

FIG. 6. (Color online) Theoretical line emission cross sections after single electron capture in 1 keV/amu collisions of O^{8+} and Ne^{10+} collisions on H_2O. The experimental data of Greenwood *et al.* at 7 q keV have been normalized to the mCTMC absolute values at the Ly α peak.

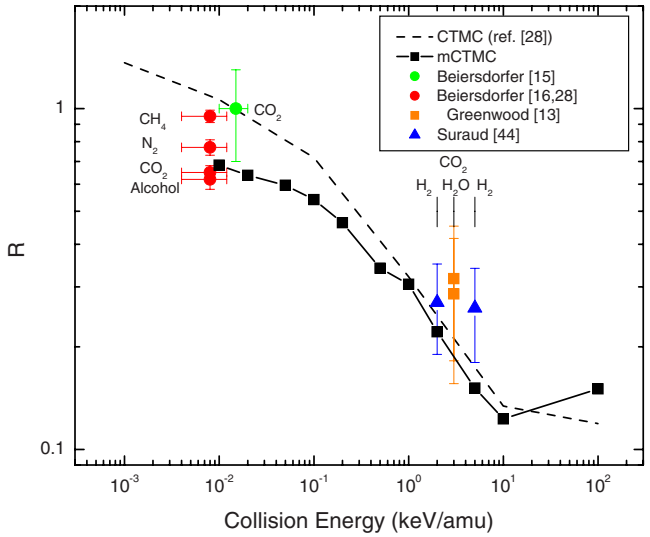

FIG. 7. (Color online) Hardness ratio for O^{8+} projectiles as a function of the impact energy. Theoretical results are presented for H_2O target. Experimental data shown are those of Beiersdorfer at 15 eV/amu [16,28], Greenwood *et al.* at 3 keV/amu [13], and Suraud at 2 and 5 keV/amu [44].

accurately predict the line emission cross sections. To illustrate this point, we show the l-state distributions at, or near, the dominant n level for the O^{8+}, Ar^{18+}, and Fe^{26+} projectiles in Fig. 5 at three impact energies of 0.01, 1, and 100 keV/amu. We display the $n=5$ state for O^{8+}, $n=10$ for Ar^{18+}, and the $n=13$ state for the Fe^{26+} projectile. At the lowest impact energies considered, it can be seen that the distributions peak at low l states (2, 3, and 4, respectively). However, the maxima of the distributions rapidly shift to higher l values as the impact energy is increased. We should note that if the collision energy is pushed to even higher energies where ionization, not electron capture, dominates the target electron removal process, the capture process reverts back to the population of low l values. This is because at very high energies the capture process is determined by velocity vector matching between projectile and target electron, resulting in preferential capture of electrons with high eccentricities. The captured electron tends to preserve its eccentricity after the capture event, thus leading to enhanced population of low l-quantum levels.

In Fig. 6, we compare our present results at 1 keV/amu to the JPL line emission cross sections [13] for O^{8+} and Ne^{10+} collisions on H_2O. The theoretical results have been corrected to take into account the photon Be window transmission and the energy resolution of the 102 eV FWHM Ge detector used in the experiments.

The present results compare well with the data. Since the data are relative, we have normalized them to our absolute line emission cross section at the Lyman alpha peak. We observe some underestimation of the $3p \rightarrow 1s$ transition for both projectiles, which is a signature of our neglect of the double capture followed by single electron Auger emission. We expect that the inclusion of the latter process would improve the comparison not only to the Ly β line, but also to the low energy side of the Ly α peak where the data provide additional evidence of autoionizing double capture [26].

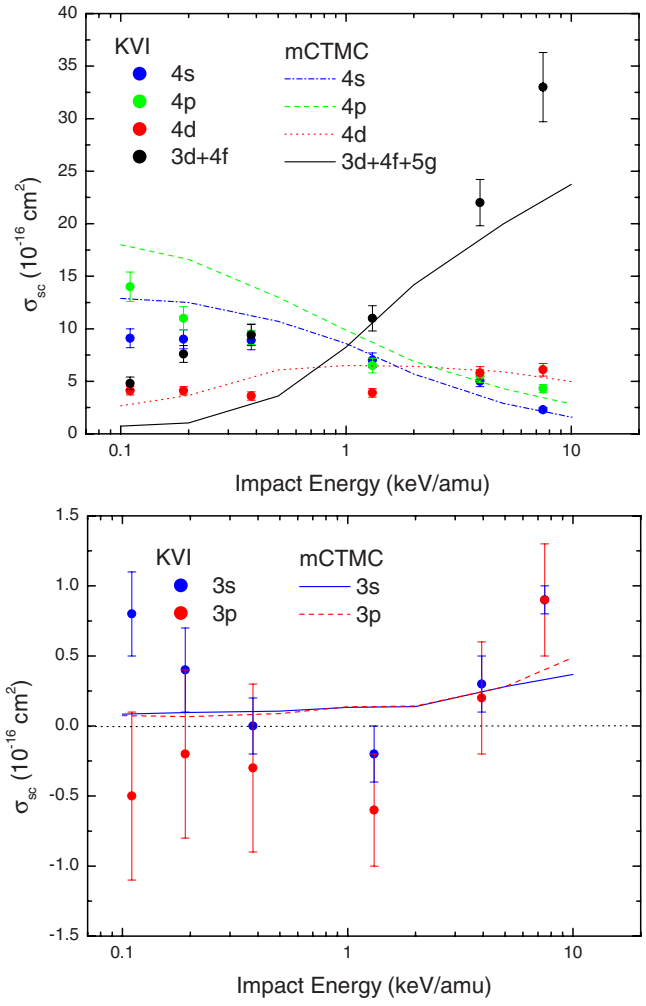

FIG. 8. (Color online) Single electron capture partial nl cross sections for O^{6+} collisions on H_2O as a function of collision energy.

The JPL experimental data for x-ray emission only exist at one collision energy. Thus, in order to test our predictions about the energy dependence of the l values against data, we must resort to a quantity termed the "hardness ratio." In Fig. 7, we present the "hardness ratio" R, defined as the line emission cross sections for the $np \rightarrow 1s$, $n>2$, divided by that for the Ly α $2p \rightarrow 1s$ value. Sufficient data only exists for the O^{8+} system.

In order to extend the energy range of the comparison, we have included data from LLNL for molecular targets with similar ionization potentials to that of H_2O since this specific system was not investigated at LLNL. Compared to our previous results, the mCTMC model corrects the overestimation of the LLNL data at the lower energies and still provides a reasonable agreement with the JPL data at impact energies around 3 keV/amu. The rise of the hardness ratio with decreasing energy provides direct evidence of the increasing population of the low l-values shown above. On the other hand, the rise shown at the highest energy considered can be ascribed to the fact that the captured electron tries to preserve its eccentricity, as already mentioned above, enhancing the population of low l levels.

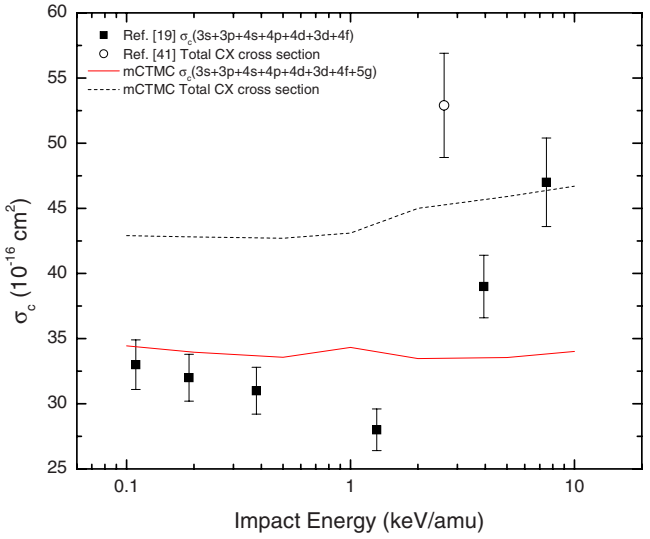

FIG. 9. (Color online) Total electron capture cross sections for O^{6+} collisions on H_2O as a function of the collision energy.

The O^{6+} system provides us with a nice opportunity to test our theoretical predictions over a relatively large energy range since absolute partial cross sections have been made available by Bodewits *et al.* [19]. The O^{6+} projectile is not fully stripped, thus we have the added uncertainty of implementing a screened potential to represent the projectile, unlike in the fully stripped projectile systems that we have considered. However, this ion has considerable relevance since O^{6+} is the most abundant solar wind ion after protons and alpha particles. It has not received attention from the astrophysical community concerning cometary photon emission since its emission energy region lies below the detection limit of the spectrometers on satellites that are used for such a task. However, when EUV observations become available, its contribution will be an important component to the spectra.

To represent the O^{6+} ion, we have used a Garvey potential derived from Hartree-Fock calculations [34]. This allows the target particles to see the nuclear charge $Z=8$ when they are close to the projectile, yet see the fully screened $Z=6$ charge at larger distances. Since the electron tends to be captured mainly to $n=4$ and 5 with minimal contributions from the s states, quantum defects play a minor role and the energies for the captured electron are similar to those obtained with a C^{6+} projectile. We note that our calculations show that the explicit consideration of the Garvey potential drastically modifies the l distributions of the captured electrons from that of an unscreened $Z=6$ Coulomb potential, and is necessary for a quantitative description of the collision.

In Fig. 8 we present the data along with our calculations. We are in agreement with the KVI data that the $n=3$ levels make very minor contributions to the spectra. This is in contrast to the TES data of Seredyuk *et al.* who find a large fraction of the single capture in the $n=3$ state. Their latter assignment is most likely due to double capture to $3l,nl$ ($n>4$) with the $n=3$ electron decaying to its ground state via Auger emission of the other electron in a higher lying level. This is supported by sample calculations at 1 keV/amu using a hydrogenic target with a binding energy of 27.5 eV (the second ionization potential for H_2O). We find that the electrons captured in such collisions mainly populate the $n=3$ state (83% of the events) and have a cross section magnitude that is approximately 16% that of capture from the ground states. Such double capture–Auger processes would not be observed in the EUV spectra. Moreover, for direct single capture, neither our calculations nor the KVI results are able to confirm the TES data indicating that the specific $O^{5+}(1s^24d)$ level dominates the single capture reaction, rather we find it is all of the $O^{5+}(1s^2n=4)$ levels.

What is surprising in both the KVI data and our calculations is the rapid rise in the $3d+4f$ cross section with collision energy. Here, the observations followed the $3d\rightarrow 2p$ transition, so that other contributions from the yrast chain must be considered. As shown in Fig. 5, the preference for population of the largest l values has a rapid energy dependence. Our calculations indicate that the extreme energy dependence is due not only to a rapid increase in the $4d$ contribution, but is also due to the $5g$ state that contributes significantly at the highest energies.

In Fig. 9, we show the total electron capture cross sections for O^{6+} collisions on H_2O. We have also plotted the partial contributions arising from the $n=3,4$ states and the $5g$ state to compare with the KVI data. Since Bodewits *et al.* obtain the capture cross sections indirectly from their line emission cross sections, they attach the discrepancy between their results and those obtained by Mawhorter at 2.6 keV/amu to autoionizing double electron capture.

Our mCTMC calculations also do not explicitly include the autoionizing double capture. Thus, our total cross section also underestimates the result of Mawhorter *et al.* On the other hand, in contrast to the KVI data, we obtain a significant number of capture events to the $O^{6+}(n=5)$ state, as can be clearly inferred from Fig. 9. Furthermore, we are unable to account for the energy dependence of the total cross section that is obtained from the EUV spectra.

CONCLUSIONS

In this paper we have presented a theoretical description of charge exchange reactions between highly charged ions with $Z=4-10$, 14, 18, and 26 colliding with H_2O molecules. The reaction was studied over a large energy interval with a range of projectile charges in order to provide information on the systematic trends of the partial cross sections along with their expected line emission spectra.

We have introduced an initialization for the active electron that provides a more accurate representation of the momentum and radial distributions for H_2O. We find that the present model improves upon the description of single electron capture total cross sections when compared to the hydrogenic-microcanonical CTMC model employed in the past. Furthermore, the l distributions of the captured electrons appear to be more accurately described as inferred from the present results for the hardness ratio.

We have also studied the collision of O^{6+} projectiles on H_2O, a system recently investigated by the KVI and the Belfast groups. We conclude that the multielectronic character of

the projectile needs to be explicitly considered. We are in general agreement with the absolute nl-partial cross sections obtained from the EUV spectra, and provide an explanation for the energy dependence of the $3d \rightarrow 2p$ photon transition. However, we are not in accord with the interpretation of the TES measurements that the $O^{5+}(4d)$ level dominates the single capture product states.

It is clear from the present analysis that further theoretical and experimental work is needed concerning multiple capture followed by Auger stabilization in collisions involving highly charged ions with the H_2O molecule.

ACKNOWLEDGMENTS

Work at UMR supported by the Office of Fusion Energy Sciences, DOE. Work at UNS supported by PGI 24/F038 and PICTR 03/0437 of the ANPCyT (Argentina).

[1] W. Fritsch and C. D. Lin, Phys. Rep. **202**, 1 (1991).
[2] N. Shimakura, S. Suzuki, and M. Kimura, Phys. Rev. A **48**, 3652 (1993).
[3] A. Salop and R. E. Olson, Phys. Rev. A **13**, 1312 (1976).
[4] R. Abrines and I. C. Percival, Proc. Phys. Soc. London **88**, 873 (1966).
[5] R. E. Olson and A. Salop, Phys. Rev. A **16**, 531 (1977).
[6] J. A. Perez, R. E. Olson, and P. Beiersdorfer, J. Phys. B **34**, 3063 (2001).
[7] R. E. Olson, K. H. Berkner, W. G. Graham, R. V. Pyle, A. S. Schlachter, and J. W. Stearns, Phys. Rev. Lett. **41**, 163 (1978).
[8] R. A. Phaneuf, Phys. Rev. A **28**, 1310 (1983).
[9] R. E. Olson, Phys. Rev. A **24**, 1726 (1981).
[10] R. K. Janev and H. Winter, Phys. Rep. **117**, 265 (1985).
[11] T. E. Cravens, Science **296**, 1042 (2002).
[12] J. B. Greenwood, I. D. Williams, S. J. Smith, and A. Chutjian, Astrophys. J. Lett. **533**, L175 (2000).
[13] J. B. Greenwood, I. D. Williams, S. J. Smith, and A. Chutjian, Phys. Rev. A **63**, 062707 (2001).
[14] P. Beiersdorfer, R. E. Olson, G. V. Brown, H. Chen, C. L. Harris, P. A. Neill, L. Schweikhard, S. B. Utter, and K. Widmann, Phys. Rev. Lett. **85**, 5090 (2000).
[15] P. Beiersdorfer, C. M. Lisse, R. E. Olson, G. V. Brown, and H. Chen, Astrophys. J. Lett. **549**, L147 (2001).
[16] P. Beiersdorfer, K. R. Boyce, G. V. Brown, H. Chen, S. M. Kahn, R. L. Kelley, M. May, R. E. Olson, F. S. Porter, C. K. Stahle, and W. A. Tillotson, Science **300**, 1558 (2003).
[17] B. Wargelin, P. Beiersdorfer, P. A. Neill, R. E. Olson, and J. H. Scofield, Astrophys. J. **634**, 687 (2005).
[18] D. Bodewits, R. Hoekstra, B. Seredyuk, R. W. McCullough, G. H. Jones, and A. G. G. M. Tielens, Astrophys. J. **642**, 593 (2006).
[19] D. Bodewits and R. Hoekstra, Phys. Rev. A **76**, 032703 (2007).
[20] B. Seredyuk, R. W. McCullough, and H. B. Gilbody, Phys. Rev. A **72**, 022710 (2005).
[21] H. Tawara, E. Takács, T. Suta, K. Makónyi, L. P. Ratliff, and J. D. Gillaspy, Phys. Rev. A **73**, 012704 (2006).
[22] F. I. Allen, C. Biedermann, R. Raktke, and G. Fussmann, J. Phys.: Conf. Ser. **58**, 188 (2007).
[23] R. Wegmann, H. U. Schimdt, C. M. Lisse, K. Dennerl, and J. Englhauser, Planet. Space Sci. **46**, 603 (1998).
[24] R. M. Häberli, T. I. Gombosi, D. L. De Zeeuw, M. R. Combi, and K. G. Powell, Science **276**, 939 (1997).
[25] T. E. Cravens, Geophys. Res. Lett. **24**, 105 (1997).
[26] Matthew Rigazio, V. Kharchenko, and A. Dalgarno, Phys. Rev. A **66**, 064701 (2002).
[27] V. Kharchenko, Matt Rigazio, A. Dalgarno, and V. A. Krasnopolsky, Astrophys. J. Lett. **585**, L73 (2003).
[28] S. Otranto, R. E. Olson, and P. Beiersdorfer, Phys. Rev. A **73**, 022723 (2006).
[29] S. Otranto, R. E. Olson, and P. Beiersdorfer, J. Phys.: Conf. Ser. **58**, 165 (2007).
[30] S. Otranto, R. E. Olson, and P. Beiersdorfer, J. Phys. B **40**, 1755 (2007).
[31] R. C. Isler and R. E. Olson, Phys. Rev. A **37**, 3399 (1988).
[32] H. Anderson, M. G. von Hellermann, R. Hoekstra, L. D. Horton, A. C. Howard, R. W. T. Konig, R. Martin, R. E. Olson, and H. P. Summers, Plasma Phys. Controlled Fusion **42**, 781 (2000).
[33] A. E. S. Green, D. L. Sellin, and A. S. Zachor, Phys. Rev. **184**, 1 (1969).
[34] R. H. Garvey, C. H. Jackman, and A. E. S. Green, Phys. Rev. A **12**, 1144 (1975).
[35] S. Schippers, P. Boduch, J. van Buchem, F. W. Bliek, R. Hoekstra, R. Morgenstern, and R. E. Olson, J. Phys. B **28**, 3271 (1995).
[36] H. A. Bethe and E. E. Salpeter, *Quantum Mechanics of One- and Two-Electron Atoms* (Springer, Berlin, 1957).
[37] L. Meng, C. O. Reinhold, and R. E. Olson, Phys. Rev. A **40**, 3637 (1989).
[38] C. O. Reinhold and C. A. Falcón, Phys. Rev. A **33**, 3859 (1986).
[39] G. Peach, S. L. Willis and M. R. C. Mc Dowell, J. Phys. B **18**, 3921 (1985).
[40] S. L. Willis, G. Peach, M. R. C. Mc Dowell, and J. Banerji, J. Phys. B **18**, 3939 (1985).
[41] R. Moccia, J. Chem. Phys. **40**, 2186 (1964).
[42] P. J. Richardson, J. H. D. Eland, P. G. Fournier, and D. L. Cooper, J. Chem. Phys. **84**, 3189 (1986).
[43] R. J. Mawhorter, A. Chutjian, T. E. Cravens, N. Djuric, S. Hossain, C. M. Lisse, J. A. MacAskill, S. J. Smith, J. Simcic, and I. D. Williams, Phys. Rev. A **75**, 032704 (2007).
[44] M. G. Suraud, R. Hoekstra, F. J. de Heer, J. J. Bonnet, and R. Morgenstern, J. Phys. B **24**, 2543 (1991).